Article

Journal of
Nanoscience and Nanotechnology
Vol. 16, 7539–7545, 2016
www.aspbs.com/jnn

Conventional and Fast Field Cycling Relaxometry Study of the Molecular Dynamics in Polymer Nanocomposites for Use as Drug Delivery Systems

Pedro. J. Sebastião[1,2], Mariana S. S. B. Monteiro[3], Luciana M. Brito[4], Elton Rodrigues[4], Fabián Vaca Chávez[1,2], and Maria Inês Bruno Tavares[4,*]

[1] *Center of Physics and Engineering of Advanced Materials, Instituto Superior Técnico, Universidade de Lisboa, 1049-001, Portugal*
[2] *Condensed Matter Physics Centre, Universidade de Lisboa, Lisbon, 21941-170, Portugal*
[3] *Faculdade de Farmácia, Universidade Federal do Rio de Janeiro, 21941-598*
[4] *Instituto de Macromoléculas Professora Eloisa Mano, Universidade Federal do Rio de Janeiro, Centro de Tecnologia, Bloco J, Cidade Universitária, Ilha do Fundão, CP 68525, Rio de Janeiro, RJ, 21945-970, Brazil*

This article presents a molecular dynamics study performed by combining conventional and fast-field cycling NMR relaxation techniques in nanocomposite systems for the optimization of drug delivery systems. The biodegradable polymers polycaprolactone, polylactide, polyvinyl alcohol and maize starch were used as base polymers and they were modified by incorporation of nanoparticles and/or cross-linking reactions, in order to understand the interaction between the bioactive molecules and the supporting matrix for a controlled drug release. Nevirapine was used as a testing bioactive drug. H spin-lattice relaxation times were measured for Larmor frequencies between 10 kHz and 300 MHz to obtain information about molecular motions in different time scales for comprehensive analysis of the possible interactions of the polymer matrices, modified nanoparticles and bioactive molecules. All systems presented some degree of crystallinity and poly-exponential decay of magnetization in the spin-lattice relaxation. The shortest spin-lattice relaxation times were assigned to the more amorphous regions and the relaxation dispersion was similar to that found in polymer melts. The effects of both nanoparticles and bioactive molecules on the molecular dynamics of the polymer matrices were clearly detected. The results show that NMR relaxometry study covers a broad range of frequencies and it is a powerful and suitable method to characterize nanocomposite systems at the molecular scale, provides information about the mobility of polymer chains and the strength of the interaction between polymers/nanoparticles. This information helps to make inferences about drug confinement level inside the systems, which can have a direct influence on the drug release. It is extremely important to know the exact drug release mechanism of bioactive molecules in a medical treatment. The main results indicated that the NMR techniques used were able to evaluate the molecular dynamics of the nanocomposites studied. It can be pointed out that PCL/clay nanocomposites containing nevirapine drug, caused a compensating effect regarding to the distribution of correlation times for the molecular segment motions and the drugs interferes in the nanomaterial molecular dynamics.

Keywords: NMR, Relaxometry, Fast Field Cycling, Polymer Nanocomposites.

1. INTRODUCTION

Polymers are used in a wide range of fields, including biomedical applications. In particular, the use of modified biodegradable polymers as transport agents for drug delivery systems has been investigated and shown to have advantages with respect to other pharmaceutical excipients, including single polymer systems.[1–3]

The interest in developing new optimized systems is impelling researchers to find ways for controlling and fine-tuning the physical and chemical properties of nanoscale systems. New polymer blends are being developed aiming at selective reinforcement of properties like phase

*Author to whom correspondence should be addressed.

stability, tailored solubility in both aqueous and organic media and specific interactions arising from the blend's chemical composition. By adjusting the degree of molecular organization, mixing biodegradable with synthetic polymers and introducing nanoparticles, as well as choosing the most suitable mixing method (melt compounding, spray drying, solution casting, phase inversion, to cite a few), many systems with enhanced properties can be produced. Proper characterization of systems at the nanoscopic level is essential. X-ray diffraction, infrared spectroscopy, thermogravimetric analysis and NMR are techniques commonly used to obtain information about different properties of these systems. Among different NMR techniques used, NMR relaxometry has proved to be a powerful tool that provides useful information on the molecular dynamics in different materials.[4–13] Multiple quantum NMR techniques have also been used to study details of the molecular dynamics in polymers.[14–16] In NMR relaxometry, the measurement of the spin-lattice relaxation time (T_1) over a broad range of Larmor frequencies (ηL) in polymer solutions and entangled polymer melts has shown that different relaxation dispersions can be observed depending on the molecular mass.[6] For polymers with molecular mass below a critical mass, M_c, molecular dynamics is usually well described by the Rouse model.[17] For molecular weights above M_c, it has been observed that due to molecular entanglement, chain dynamics can no longer be understood in terms of chain movements in a viscous media, but have to consider the topological constraints that hinder chain motions. The relaxation dispersion can, in this case, be interpreted in terms of the renormalized Rouse formalism.[18] Typically, different relaxation regimes are identified, all described by power laws, $T_1 \sim \nu_L^p$, where the exponent p is usually below 1.5.[6] The values of p are related to differences between the distributions of correlation times associated with the molecular motions subject to different constraints. Not only the molar mass of the macromolecules and working temperature affect the distribution of correlation times, they also influence aspects like chain entanglement, molecular cross-linking, hydrogen bonding and heterogeneities introduced by local crystallinity and/or the presence of dopant agents (e.g., organic or inorganic nanoparticles). Therefore, molecular motions can be used to monitor the degree of molecular order changes introduced by a variety of factors, by inspecting the changes in the power dependences observed in the spin-lattice relaxation dispersion.

In this work is presented an overview of a series of experimental results for ^{1}H spin-lattice relaxation measurement as a function of the Larmor frequency (NMRD) for a variety of semi-crystalline polymers. The biodegradable polymers polycaprolactone (PCL) and poly(lactic acid) (PLA), as well as the biocompatible poly(vinyl alcohol) (PVA) and maize starch, were used as base polymers and some of them were modified by incorporation of nanoparticles and/or cross-linking reactions, in order to enhance their mechanical properties, increase stability against degradation, and optimize other parameters for pharmaceutical purposes.[19–22] NMRD results were obtained for the frequency range 10 kHz–300 MHz and X-ray results are presented to characterize the degree of crystallinity of the base systems.

2. EXPERIMENTAL DETAILS

2.1. Preparation of Starch/Clay Samples

Commercial maize starch was dispersed in deionized water (2.5% by weight [w/w]) during 24 h at room temperature. Adequate amounts of nanofiller (Viscogel® B8 clay, containing dialkyldimethyl ammonium chloride as intercalant, Laviosa Chimica Mineraria S.p.A, Italy), sufficient to prepare 5% (w/w of starch) hybrids, were added to a starch dispersion at the beginning of the process. Those samples were then thermally gelatinized and poured into plastic Petri dishes to cast starch and starch/Viscogel® B8 clay films after slow water evaporation at room temperature under a fume hood.

2.2. Preparation of Nevirapine/PCL Samples

PCL pellets, Mw: 80,000–100,000 $g \cdot mol^{-1}$, supplied by Sigma-Aldrich, were dissolved in chloroform ($CHCl_3$, from Vetec, Brazil), under magnetic stirring for 48 h, in sufficient amount to yield a 5% (w/v) solution. 200 mg of nevirapine (NVP) (10% w/w in relation to PCL), supplied by Oswaldo Cruz Foundation (Rio de Janeiro, Brazil) was dispersed in sufficient amount of $CHCl_3$ under magnetic stirring for 1 h and added to the 5% (w/v) PCL solution.

Polymer-clay nanocomposites were also prepared employing commercial organomodified montmorillonite clay (Viscogel® S7, containing dialkyldimethyl ammonium chloride as intercalant, obtained from Laviosa Chimica Mineraria S.p.A, Italy) dispersed in $CHCl_3$ for 48 h under magnetic stirring. Sufficient amounts of Viscogel S7 to yield 5% (w/w of PCL) hybrids were used. Also, samples comprising PCL/Viscogel S7 with 10% NVP were obtained. All dispersions were poured into glass Petri dishes, covered and left in an oven at 40 °C until the solvent evaporated, for recovery of free-standing polymeric films. The detailed procedure is described elsewhere.

2.3. PVA, Cross-Linked PVA and PVA/Silicon Dioxide Preparation

PVA (99 + % hydrolyzed), Mw: 89,000–98,000 $g \cdot mol^{-1}$, tetraethyl orthosilicate (TEOS) (98%), and glutaraldehyde (GA) (25% m/m in H_2O) were supplied by Sigma-Aldrich. Hydrochloric acid (HCl) (37% w/w) was procured from Vetec, Brazil.

40-mL aliquots of a previously prepared 10% (by weight) aqueous PVA solution were used to obtain the samples, one each for neat PVA, cross-linked PVA and PVA/silicon dioxide (SiO_2) hybrid. To the last two

PVA solutions, a sufficient volume of a 1 $mol \cdot L^{-1}$ HCl solution was added to bring the system's pH to 2.0 ± 0.1. Then, a volume of either GA or TEOS sufficient to induce 1% nominal cross-linking or to give 1% SiO_2, based on the molar mass of the PVAs repeating unit, was added to the acidified solutions. Finally, the contents of the aliquots were poured into polystyrene Petri dishes, covered and left under a fume hood at room temperature for five days in order to allow completion of the chemical reactions. After this period, the gels were thoroughly washed with deionized water and put in a vacuum oven at 45 °C for 2 days. All the materials were stored in a desiccator under vacuum until analyses.[6]

2.4. NMR Measurements

NMR measurements were made using different experimental setups in a complementary way to cover a wide range of Larmor ^{1}H frequencies, from 10 kHz to 300 MHz. For frequencies above 9 MHz, a Bruker BE30 variable field magnet and a Bruker Avance II console were used together with a fixed field magnet and dedicated Maran console working at 23 MHz. The measurements at 300 MHz were made with a Bruker 7T superconductor magnet using an Avance II NMR console. The measurements for frequencies below 9 MHz were made using a lab-developed fast field cycling (FFC) relaxometer.[23] The T_1 times for frequencies above 9 MHz where measured using the standard inversion-recovery pulse sequence with phase cycling for bias and offset compensation. The measurements using the FFC relaxometer were carried out following the simple $B_{pol} \rightarrow B_{evo} \rightarrow \tau \rightarrow B_{evo} \rightarrow B_{pol} \rightarrow rf \rightarrow$ FID formula, where rf is the radio-frequency pulse, FID is the free induction decay, and B_{pol} and B_{evo} are the polarization and evolution magnetic fields, respectively. The T_1 length depends on B_{evo} (e.g., $\nu L = \gamma B_{evo}/(2\pi)$), while the free induction decay signal is obtained for the larger magnetic field B_{pol} for good signal-to-noise ratio measurement.[6] All values of proton relaxation times were a median of 4 measurements for each determination and the error among them was about 2%.

2.5. X-ray Diffraction

The X-ray measurements were obtained with a Rigaku D/Max 2400 diffractometer, with nickel-filtered CuKα radiation with 1.54 Å wavelengths, operating at 40 KV and 30 mA. The 2θ scanning range was varied from 2° up to 40°, with 0.02° steps, at room temperature.

3. RESULTS AND DISCUSSION

Figure 1 presents the ^{1}H spin-lattice relaxation time curves as a function of the Larmor frequency for the base polymer systems involved in the work: PLA, PCL, PVA, and starch.

As can be observed in Figure 1, the T_1 is longer for the PLA (pellets) in comparison with the other polymers for frequencies below 80 MHz, due to the chemical

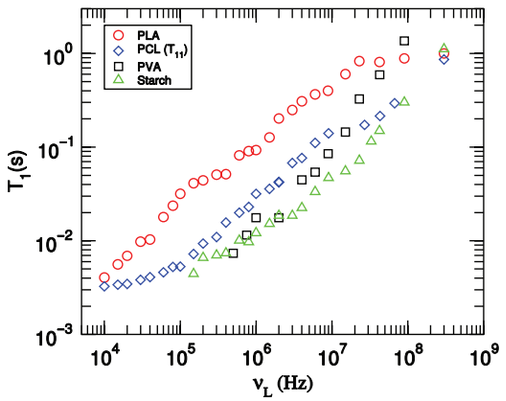

Figure 1. ^{1}H spin-lattice relaxation time curves as a function of Larmor frequency for the base polymer systems: PLA pellets, PCL pellets, PVA film and starch film.

structure and intermolecular interactions between polymer chains. The spin-lattice relaxation dispersion profile for PCL presents lower values in comparison with PLA, which means that the intermolecular interactions in this polymer have different forces compared with PLA that comes from the molecular organization of the PCL chains. Clearly, the T_1 profiles for the PVA and starch are below the other two polymers. Since the spin-lattice relaxation time data refer to pure polymer, it is reasonable to consider that higher T_1 values correspond to longer correlation times in relation to slower motions, showing that these polymers have different chain molecular organization and consequently intermolecular interaction. These intermolecular interactions exert distinct forces on the configuration of polymer chains according to the spatial proximity between chains and relaxation process behavior; the measurements of relaxation time are sensitive to domains formed with size ranging from 25 to 50 nm.

Figure 2 presents the X-rays diffraction profiles for the base polymers: PCL pellets, PLA pellets, neat PVA and neat starch films. As can be observed in this Figure, the base polymer systems studied have different degrees of local molecular organization. PCL and PLA-pellets present

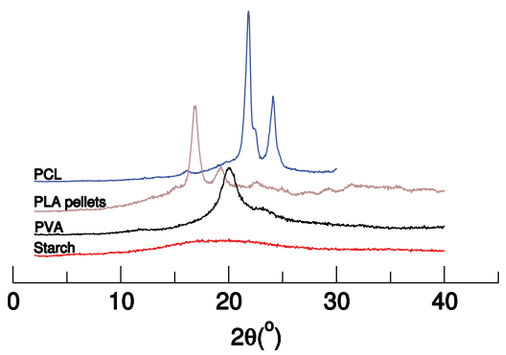

Figure 2. X-ray diffraction profiles obtained for the base polymer systems: PCL pellets, PLA pellets, neat PVA and neat starch films.

sharper X-ray peaks at large angles that overlap the usual broad peak associated with the lateral molecular packing disorder. Both starch and PVA film systems present amorphous local packing. The PVA does not form crystallites, but the chains present some molecular organization, which varies according to the degree of hydrolysis. The physical ordering displayed by the polymer in its diffraction pattern arises because of the small size of the hydroxyl side group, allowing inter/intramolecular hydrogen bonding and leading to more efficient packing of the polymer chains.[24] The PCL and PLA pellet systems are therefore semicrystalline systems where high packed polymer molecules form small crystals, which in the end might affect the molecular dynamics of the whole system. These results show that in film form, the molecular chain organization is different, which influences the molecular movement (mobility) of the chains. The informations obtained from X-ray are in accordance with NMR relaxation parameter showed in Figure 1.

Figure 3 depicts the T_1 experimental results for modified PVA and starch polymer systems. In the case of PVA, 1% (w/w) of silica particles was incorporated in a sol–gel chemical procedure. In the case of starch, containing 5% (w/w) of organophilic clay (Viscogel B8), they were mixed during preparation of the films. The experimental results in both situations showed that the inclusion of nanoparticles in the systems promotes change in the T_1 parameter according to the dispersion of the profile, which slows down the decrease of T_1 along frequency, due to the formation of new and strong intermolecular interactions between the polymer chain and nanoparticles; these new and stronger interactions are formed between nanoparticle and polymer chains, because the polymer–polymer interaction are broken and the nanoparticle are not agglomerated. In the case of these nanocomposites, the presence of intimately mixed nanoparticles-polymer domains causes an increase of T_1 because of the reduction of degrees freedom for the composites when compared to neat polymers.

Figure 4 shows the experimental T_1 results for PCL and modified PCL systems. The PCL nanocomposites were prepared with addition of 5% (w/w) of montmorillonite clay Viscogel S7 and NVP, a drug which is used in human immunodeficiency virus (HIV) therapy. It is interesting to note that in the case of the PCL samples, the magnetization decay used to measure the spin-lattice relaxation was tri-exponential instead of mono-exponential, as observed for the other systems. This observation is consistent with the fact that this polymer is clearly semi-crystalline, as can be observed from the X-ray diffraction profiles. The relative contributions of the magnetization decay are in agreement with the relative crystalline weights obtained from the areas of the X-ray diffraction peaks at large angles, as observed in Figure 2. Three regions can be identified: one associated with the more "rigid" PCL crystallites, a second one associated with a rigid-amorphous molecular packing and a third one flexible—amorphous region and possible association with the chain molecular terminal segments. Because the three relaxation times (T_{11}, T_{12}, and T_{13}) that describe the magnetization decay are affected by the presence of the nanoparticles, it is possible to infer that the dispersion of the nanoparticles, including the S7 clay and NVP, affect molecular motions in all PCL domains. A detailed analysis of the dispersion curves shows that the presence of clay nanoparticles and NVP molecules tend to produce effects on the PCL matrix that cancel out to some extent. In fact, the presence of NVP tends to compensate for the increase in T_{11} observed by addition of Viscogel S7 (see Fig. 4). This is produced by the change in material crystallinity and also in the intermolecular forces and interactions created through the formation of the composites, as a consequence good dispersion and distribution of the nanoparticles in the polymer matrix were observed, generating mixing materials containing part exfoliated and part intercalated.

All dispersion profiles presented are well described with frequency dependence power law, $T_1 \sim \nu_L^p$.

Figure 5 shows the power law fits in the frequency regions of the maize starch systems. It is interesting to note that the exponents for the maize starch nanocomposite are smaller than those obtained for pure maize starch,

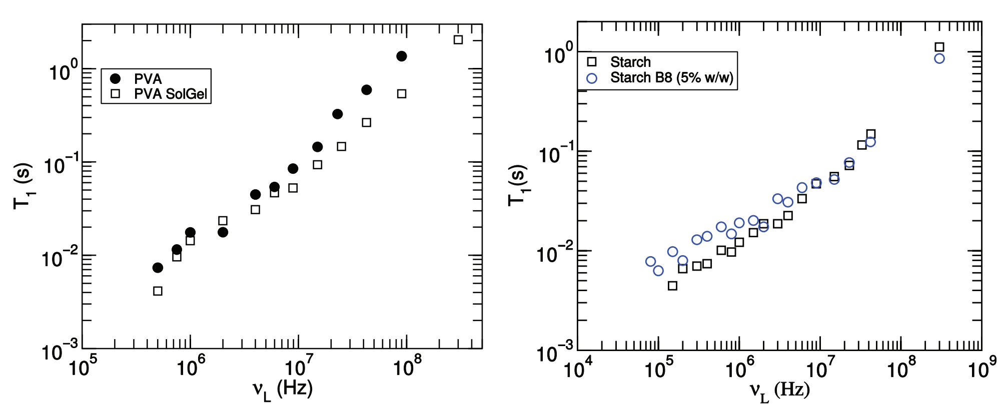

Figure 3. [1]H spin-lattice relaxation time as a function of the Larmor frequency for modified PVA and starch polymers, as explained in the text.

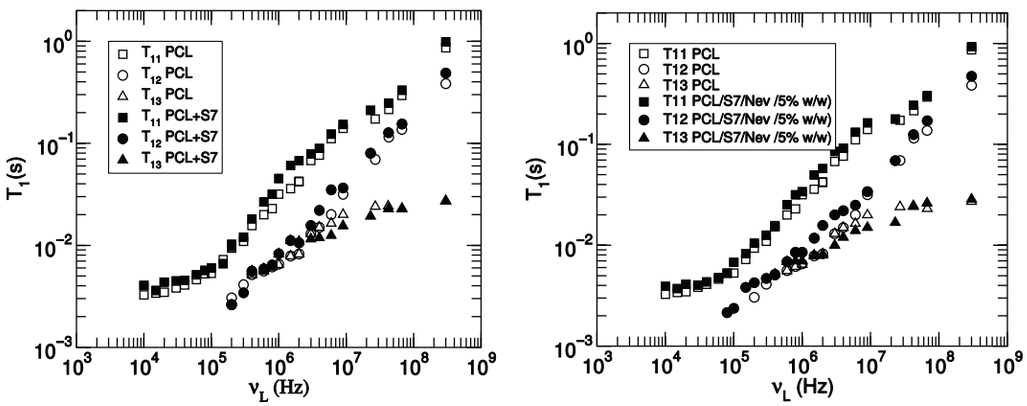

Figure 4. ^{1}H spin-lattice relaxation time as a function of the Larmor frequency for modified PCL and modified PCL systems, as explained in the text.

indicating possible exfoliation of the inorganic clay layers and intercalation of starch macromolecules between the layers, with a consequent decrease in mobility and increase in T_1 for low frequencies (below ~10 MHz). Figure 6 presents the power law T_1 fits for the tri-component PCL/S7/NVP sample. As can be observed, the three spin-lattice components are well fitted by power law frequency dependencies with different exponents in different regions. Therefore, the distribution of correlation times for molecular motions is different for each molecular organization domain. Also, the addition of nanoparticles to the PCL system has different effects on the distribution of correlation times for the segmental motions, depending on the degree of molecular mobility in each domain, as can be seen by comparing the results in Figure 5 with those obtained for PCL.[25] The large values of the power law exponents for the T_{11} and T_{12} relaxation components close to 0.75 might indicate that molecular segment motions occur in a highly local ordered medium, which is derived from the new PCL systems formed, taking into consideration that the nanoparticles and drugs are well dispersed and distributed in the polymer matrix.

Figure 7 presents the T_1 fits of the PVA based systems and also a fit from Kimmich et al.[26] for a polybutadiene cross-linked polymer to compare the relation of the molecular movements, employing the same fit, due to the correlation behavior found between those, according to the similarity effect caused by both methods.

Figure 7(a) shows that the addition of silica nanoparticles to the PVA polymer produces a change in the molecular dynamics PVA ^{1}H spin-lattice relaxation times data match significantly well with the crosslinked polybutadiene polymer data, taking into account the values of the fitting exponents. Moreover, the crosslinking in the PVA system produces a similar effect on the molecular dynamics to that associated with the addition of silica particles. In fact, the T_1 dispersion and power law fits of the crosslinked PVA systems (P1) is very similar to that observed for the polybutadiene system, showing that the polymer nanocomposite systems behave like crosslinked

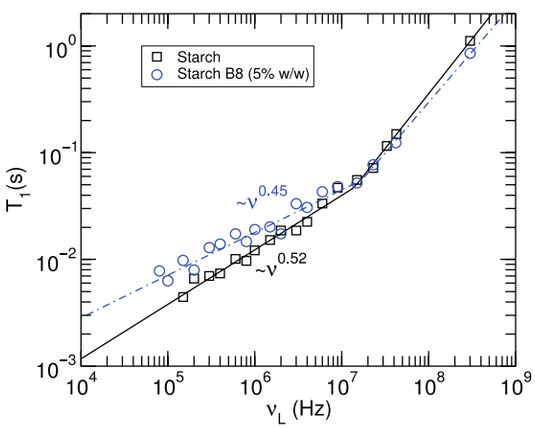

Figure 5. ^{1}H spin-lattice relaxation time as a function of Larmor frequency for starch polymer systems, as explained in the text. The exponents of the power laws above $\nu_{I,II} \sim 17$ MHz were 1.05 and 0.87 for the starch and starch/B8 systems, respectively.

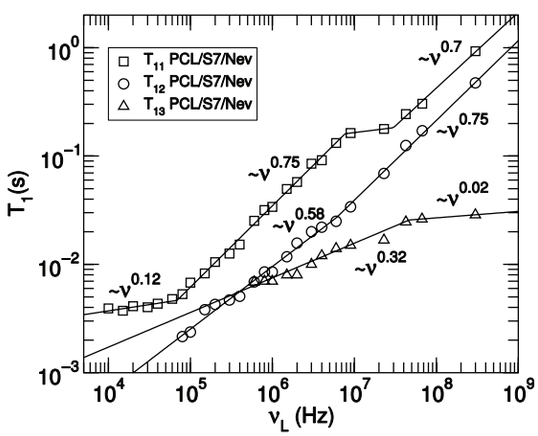

Figure 6. ^{1}H spin-lattice relaxation time as a function of Larmor frequency for modified PCL polymer systems, as explained in the text. The fitted power law curves and respective exponents.

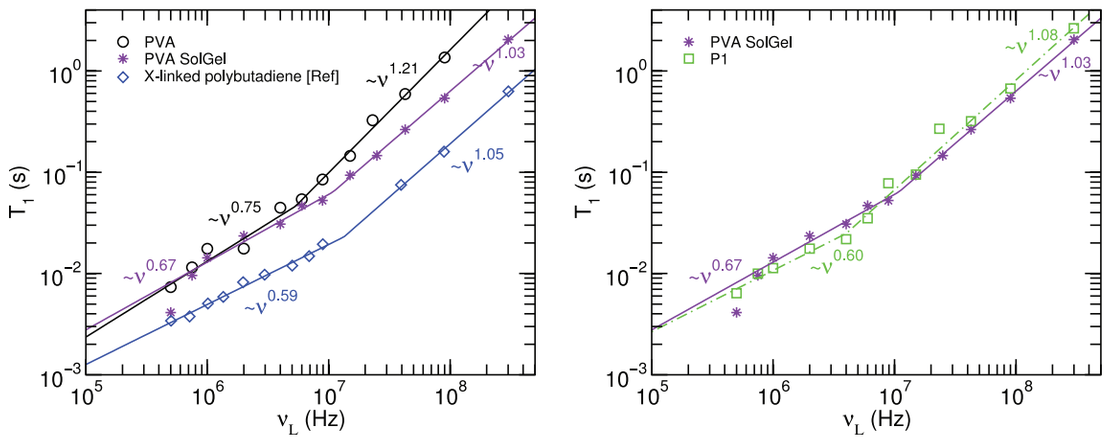

Figure 7. ^{1}H spin-lattice relaxation time as a function of Larmor frequency for modified PVA polymer systems, as explained in the text. For comparison purposes, the crosslinked polybutadiene data come from research by Kimmich et al.[6]

materials. This fact can be related to the dispersion and distribution mode of the nanoparticles, especially the clay lamellae, which when dispersed can assume different conformations (morphologies) such as exfoliated and intercalated. Mixture of these morphologies promotes different intermolecular forces due to the restriction of the polymer chain movements, as was shown by the decrease in the relaxation measurements. Therefore, NMR relaxometry proved to be a good technique to evaluate the molecular dynamics of polymer nanocomposites.

4. CONCLUSIONS

The comparative study of the molecular dynamics in different biocompatible polymer systems modified by inclusion of nanoparticles and/or molecular cross-linking showed that both inorganic (silica, clay) particles and molecules with pharmaceutical properties, like nevirapine, were well dispersed and distributed in the polymer matrices, promoting changes in the molecular order at local scale and on the molecular dynamics, according to the changes detected in the relaxation parameter, promoted by the intermolecular interactions causing nanoparticles dispersion and distribution.

The data on molecular mobility, obtained from measurements of the proton NMR spin-lattice relaxation times over a broad range of Larmor frequencies (10 kHz–300 MHz), were correlated with data on the local molecular organization from X-ray diffraction. Some of the nuclear magnetization of the semi-crystalline compounds presented a multi-exponential decay, due to the formation of domains with different molecular mobility, and different spin-lattice relaxation times could be estimated corresponding to regions with different degrees of crystallinity, as obtained from the X-ray diffraction peak areas. In all systems, the power law spin-lattice relaxation time dependency on frequency could be used to fit the experimental results, enabling distinguishing between different types of modifications of a given base polymer, as in the case of PVA samples. The inclusion of clay nanoparticles and nevirapine in some of the systems may cause a compensating effect regarding distribution of correlation times for the molecular segment motions.

From the results obtained, it can be pointed out that proton NMR relaxometry is a sensitive method to study small perturbations of a polymer matrix by the addition of different nanoparticles and/or molecular crosslinking agents, including molecules with important pharmaceutical properties, thus contributing to the optimization of systems for controlled drug release for medical treatment.

Acknowledgments: We thank the Brazilian funding institutions CAPES, CNPQ and FAPERJ for their financial support, and the Portuguese FCT project UID/CTM/04540/2013.

References and Notes

1. C. B. Dornelas, C. R. Rodrigues, S. S. Coutinho, H. C. Castro, L. R. S. Dias, V. P. Sousa, and L. M. Cabral, *J. Pharm. Pharm. Sci.* 14, 17 (**2011**).
2. H. V. A. Rocha, A. S. Gomes, C. B. Dornelas, F. A. Carmo, C. R. Rodrigues, H. Castro, T. S. Santos, and L. M. Cabral, *Polym.—Plast. Technol.* 47, 1256 (**2008**).
3. A. M. Júnior, F. A. Carmo, L. M. Cabral, M. I. B. Tavares, A. S. Gomes, L. A. M. Grillo, and C. B. Dornelas, *Int. Res. J. Pharm. Pharmacol.* 1, 55 (**2011**).
4. R. Dong, Nuclear Magnetic Resonance of Liquid Crystals, Springer-Verlag, New York (**1997**) p. 14.
5. R. Y. Dong, Nuclear Magnetic Resonance Spectroscopy of Liquid Crystals, World Scientific, Singapore (**2010**).
6. R. Kimmich and E. Anoardo, *Progr. NMR Spectrosc.* 44, 257 (**2004**).
7. L. A. Neves, P. J. Sebastião, I. M. Coelhoso, and J. G. Crespo, *J. Phys. Chem. B* 115, 8713 (**2011**).
8. M. Vilfan, T. Apih, P. J. Sebastião, G. Lahajnar, and S. Zumer, *Phys. Rev. E* 76, 0517081 (**2007**).
9. P. J. Sebastião, A. Gradisek, L. F. V. Pinto, T. Apih, M. H. Godinho, and M. Vilfan, *J. Phys. Chem. B* 115, 14348 (**2011**).
10. T. Apih, V. Domenici, A. Gradisek, V. Hamplová, M. Kaspar, P. J. Sebastião, and M. Vilfan, *J. Phys. Chem. B* 114, 11993 (**2010**).

11. F. V. Chávez, P. J. Sebastião, Y. Miyake, H. Monobe, and Y. Shimizu, *J. Phys. Chem. B* 116, 2339 (**2012**).
12. P. J. Sebastião, D. Sousa, A. C. Ribeiro, M. Vilfan, G. Lahajnar, J. Seliger, and S. Zumer, *Phys. Ver E* 72, 0617021 (**2005**).
13. M. S. M. Preto, M. I. B. Tavares, P. J. O. Sebastião, and R. B. V. Azeredo, *Food Chemistry* 136, 1272 (**2013**).
14. F. V. Chávez and K. Saalwächter, *Phys. Rev. Lett.* 104, 198 (**2010**).
15. F. V. Chávez and K. Saalwächter, *Macromolecules* 44, 1549 (**2011**).
16. F. V. Chávez and K. Saalwächter, *Macromolecules* 44, 1560 (**2011**).
17. P. E. Rouse, *J. Chem. Phys.* 21, 1272 (**1953**).
18. M. Doi and S. F. Edwards, The Theory of Polymer Dynamics, Clarendon, Press, Oxford (**1986**).
19. L. M. Brito and M. I. B. Tavares, *J. Nanosci. Nanotechnol.* 12, 4508 (**2012**).
20. M. S. S. B. Monteiro, C. L. Rodrigues, R. C. Neto, and M. I. B. Tavares, *J. Nanosci. Nanotechnol.* 12, 7307 (**2012**).
21. A. Paudel, M. Geppi, and G. Van den Mooter, *J. Pharm. Sci.* 103, 2635 (**2014**).
22. H. E. Miltner, N. Watzeels, N. A. Gotzen, A. L. Goffin, E. Duquesne, S. Benali, B. Ruelle, S. Peeterbroeck, P. Dubois, B. Goderis, G. V. Assche, H. Rahier, and B. V. Mele, *Polymer* 53, 1494 (**2012**).
23. D. M. Sousa, G. D. Marques, J. M. Cascais, and P. J. Sebastião, *Solid State NMR* 38, 36 (**2010**).
24. H. S. Mansur, R. L. Oréfice, and A. A. P. Mansur, *Polymer* 45, 7193 (**2004**).
25. M. S. S. B. Monteiro, F. V. Chávez, P. J. Sebastião, and M. I. B. Tavares, *Polym. Test* 32, 553 (**2013**).
26. R. Kimmich, K. Gille, N. Fatkullin, R. Seitter, S. Hafner, and M. Müller, *The Journal of Chemical Physics* 107, 5973 (**1997**).

Received: 16 September 2015. Accepted: 13 October 2015.